

# An Approach to Using Agricultural Waste Fibres in Biocomposites Application: Thermogravimetric Analysis and Activation Energy Study

M. Siti Alwani,<sup>a</sup> H.P.S. Abdul Khalil,<sup>a,b,\*</sup> O. Sulaiman,<sup>a</sup> Md Nazrul Islam,<sup>a,c</sup> and Rudi Dungani<sup>a,d</sup>

Thermal stability behaviour of coconut coir, banana pseudo stem, pineapple leaf, and sugarcane bagasse fibres was investigated under nitrogen atmosphere. The parameters of degradation kinetics were determined by thermogravimetric analysis at heating rates of 5, 10, 15, 20, 30, and 40 °C/min using the Kissinger, Flynn-Wall-Ozawa and Friedman model-free methods. Thermal degradation of these fibres showed both two and three mass loss steps attributed from the moisture evaporation and to the decomposition of cellulose, hemicelluloses, and lignin as well as other organic materials. The results also showed that activation energy was an increasing function of conversion ( $\alpha$ ), and an apparent activation energy of 75 to 200 kJ/mol was found for most of the fibres throughout the polymer processing temperature range. These findings are significant for developing a fundamental approach to understand the thermal decomposition behaviour of agricultural waste fibres in the course of biocomposite and bio-ethanol production.

*Keywords: Biomass; Kinetic analysis; Kissinger; Flynn-Wall-Ozawa; Friedman*

*Contact information: a: School of Industrial Technology, Universiti Sains Malaysia, 11800, Penang, Malaysia; b: Department of Biocomposite Technology, Institute of Tropical Forestry and Forest Products (INTROP), Universiti Putra Malaysia, 43400 UPM Serdang, Selangor, Malaysia; c: School of Life Science, Khulna University, Khulna – 9208, Bangladesh; d: School of Life Sciences and Technology, Institut Teknologi Bandung, Gedung Labtex XI, Jalan Ganessa 10, Bandung 40132, West Java-Indonesia; \* Corresponding author: akhalilhps@gmail.com*

## INTRODUCTION

Rising environmental concerns related to raw materials, costs of raw materials for the supplied products in the market, shortages of woody materials, and concerns regarding the sustainable resource management necessitate alternative sources for lignocellulosic biomass in the wood-based industries. The use of agricultural and agro-industrial residues and non-wood plants could contribute to reduce the large amount of wood used as feedstock by the wood-based industries and would preserve and maintain the environment without much destruction. In recent years, natural fibres from non-wood materials in the form of fibres and/or particles have received attention by different wood-based industries. As natural lignocellulosic polymer materials, they are subjected to thermal degradation during many industrial processes such as composites fabrication and bio-ethanol production (Slopiecka *et al.* 2012). It is thus of practical significance to understand and predict the thermal decomposition process of these natural polymers, and the knowledge would help better design final products by estimating the influences on product properties. Pyrolysis of natural biomass fibres has received much recent interest because it can produce liquid yield up to 75% wt on a dry-feed (Guillain *et al.* 2009). It is

one of the first steps of all thermochemical processes that occur in an inert atmosphere (Fantozzi *et al.* 2009) influenced by heating rate, temperature, pressure, residence time, moisture, composition of biomass, and size of particles. Thermogravimetric analysis (TGA) is the most common technique used for kinetic analysis of the devolatilisation process, and it provides the possibility of evaluating the mass loss of a sample with temperature and time (White *et al.* 2011). Solid state kinetic data from TGA can be analysed by various methods (Sbirrazzuoli *et al.* 2009) either by model-fitting or model-free methods. Model fitting methods consist of fitting different models to the data for getting the best statistical fit model from which the kinetic parameters are calculated. The model-free methods require several kinetic curves to perform the analysis without making any assumptions about the reaction function and reaction order. Using a variety of computational methods, researchers (Cabrales and Abidi 2010; Słopiecka *et al.* 2012) observed that isoconversional and multi-heating methods can be particularly useful in describing kinetics of complex material reactions. The advantages of this approach is its simplicity; also, it could avoid the risk of choosing the wrong kinetic model and therefore, obtaining wrong kinetic parameters (Yao *et al.* 2008; Opfermann *et al.* 2002). Therefore, the multiple heating rate methods such as that of Kissinger, Friedman and Flynn-Wall-Ozawa are the most common methods used (Lu *et al.* 2009; Arora *et al.* 2011; Sathasivam and Haris 2012). These methods are increasingly being adopted in thermo-chemical conversion research of biomass fibres and allow the estimation of activation energy ( $E_a$ ). Słopiecka *et al.* (2012) examined the kinetic study of the pyrolysis of poplar wood by a comparison of Kissinger and FWO methods with a good agreement value of 153.92 kJ/mol and 158 kJ/mol, respectively. Corradini *et al.* (2009) studied the activation energy of several cotton fibres with TG and Flynn-Wall-Ozawa method, and it was around 150kJ/mol. They concluded that these methods were efficient in the description of the degradation mechanism of solid state reactions.

Malaysia produces a vast amount of agricultural waste (47,402 dry kiloton/year (Goh *et al.* 2010), and most of it originates from oil palm industries (Sumathi *et al.* 2008). However, the amount of waste from sugarcane, coconut, pineapple, and banana plants are also notably high, and wood-based industries have also shown interest in these fibres in recent years. Numerous studies (White *et al.* 2011; Wielage *et al.* 1999; Ishak *et al.* 2012; Sathasivam and Haris 2012) were conducted to investigate the thermal analysis of various types of biomass fibres. However, very limited research has been done on tropical agricultural waste fibre, especially concerning sugarcane bagasse (SCB), coconut husks (COIR), pineapple leaf (PALF), and banana pseudo stem (BPS) fibres. Moreover, the reported kinetic parameters of these natural fibres have been in wide ranges because of different kinetic schemes and variations in raw materials from different regions used for the studies. The activation energy obtained by other researchers for bagasse ranged from 87 to 225 kJ/mol (Munir *et al.* 2009; Aboyade *et al.* 2011), whereas it ranged between 149 and 210 kJ/mol for banana fibres (Sathasivam and Haris 2012). In general, the decomposition of plant fibres occurs in two to four stages of weight loss at 25 °C to 800 °C, depending on the types and sources of natural fibres (Brígida *et al.* 2010). Sathasivam and Haris (2012) reported the effect of temperature on chemical modification of banana pseudostem fibres. They found that the banana fibre started to degrade at 271 °C with maximum degradation at 320 °C. Ishak *et al.* (2012) reported four phases of decomposition of the oil palm fibres, starting with moisture loss, and followed by successive decomposition of hemicelluloses, cellulose, and lignin in the ranges of 45 to

123, 210 to 300, 300 to 400, 160 to 900, and 1723 °C, respectively. According to Mothé and Miranda (2009), thermal degradation of sugarcane bagasse and coconut fibre had two mass loss steps, where sugarcane bagasse had higher thermal stability compared to coconut coir fibres.

The purpose of this work was to investigate the kinetics of thermal decomposition of different agricultural wastes fibres, *i.e.*, SCB, COIR, PALF, and BPS. The pyrolysis process was performed by TGA, and the thermal analysis curves were recorded at several linear heating rates. Three model-free non-isothermal methods were used to calculate the activation energy ( $E_a$ ). This study would help to explore energy potentials and find out new avenues of these biomass fibres for various applications.

### Theoretical Approach

The pyrolysis process can generally be described as,



where volatile is the sum of gas and tar and  $k$  is the rate constant of reaction whose temperature dependence is expressed by the Arrhenius equation (Eq. 2),

$$k = A e^{\frac{-E_a}{RT}} \quad (2)$$

where  $E_a$  is the activation energy ( $\text{kJ mol}^{-1}$ ),  $T$  is the absolute temperature in Kelvin (K),  $R$  is the gas constant ( $8.314 \text{ J K}^{-1} \text{ mol}^{-1}$ ), and  $A$  is the pre-exponential factor ( $\text{min}^{-1}$ ). The most commonly used equation to describe the reaction rate in the non-isothermal decomposition kinetics is presented as Eq. 3,

$$\frac{d\alpha}{dt} = k(T)f(\alpha) \quad (3)$$

where  $\alpha$ ,  $t$ ,  $k(T)$ , and  $f(\alpha)$  represent the degree of conversion, time, rate constant, and reaction model, respectively. The conversion rate ( $\alpha$ ) can be calculated according to Eq. 4,

$$\alpha = \frac{m_i - m_a}{m_i - m_f} \quad (4)$$

where  $m_i$  is the initial mass of the sample,  $m_a$  is mass at time  $t$ , and  $m_f$  is the final mass.

Combination of equations 2 and 3 gives the fundamental expression of analytical methods to calculate the kinetic parameters, which is expressed in Eq. 5.

$$\frac{d\alpha}{dt} = A \cdot f(\alpha) \cdot e^{\frac{-E_a}{RT}} \quad (5)$$

For a dynamic TGA process, introducing the heating rate,  $\beta = dT/dt$  into Eq. 5, Eq. 6 can be derived:

$$\frac{d\alpha}{dT} = \frac{A}{\beta} \cdot f(\alpha) \cdot e^{\frac{-E_a}{RT}} \quad (6)$$

Equations (5) and (6) are the fundamental expressions of analytical methods to calculate kinetic parameters on the basis of TGA data.

The most common model-free methods used in this study are summarised in Table 1. In the Kissinger (1957) method,  $\ln(\beta/T_p^2)$  is plotted against  $1/T_p$  for a series of experiments at different heating rates with the peak temperature,  $T_p$ , obtained from the DTG curve. The Friedman (1964) method is the iso-conversional method, which directly leads to  $-E_a/R$  for a given value of  $\alpha$  by plotting the term  $\ln(d\alpha/dt)$  against  $1/T$ . The iso-conversional Flynn-Wall-Ozawa (F-W-O) (Flynn and Wall 1966) method is an integral method, which leads to  $-E_a/R$  from the slope of the line determined by plotting  $\log \beta$  against  $1/T$  at any certain conversion rate.

**Table 1.** Kinetic Methods Used in Calculating Activation Energy in This Study

Methods	Equation	Reference
Kissinger	$\ln \frac{\beta}{T^2} = \ln \frac{AR}{E} - \frac{E}{RT}$ (Eq. 7)	Kissinger 1957
Friedman	$\ln \frac{d\alpha}{dt} = \ln[Af(\alpha)] - \frac{E_a}{RT}$ (Eq. 8)	Friedman 1964
F-W-O	$\ln \beta = \log \left( \frac{AE}{Rg(x)} \right) - 5.331 - 1.052 \frac{E_a}{RT}$ (Eq. 9)	Flynn and Wall 1966

## EXPERIMENTAL

### Materials

Four different types of agricultural waste fibres were used in this study, viz., banana (*Musa sapientum*) fibres obtained from the pseudo stem of the plant, sugarcane (*Saccharum officinarum*) bagasse fibres, coconut (*Cocos nucifera*) husks fibres, and pineapple (*Ananas comosus*) leaf fibre. Fibres were collected from the commercial grower of these plants in Kedah, Malaysia. Samples were air dried for a week, and then oven dried at 50 °C for 48 h. Dried materials were then ground with a Wiley mill and screened. Samples of particle size between 20 and 28 mesh size were collected for the test.

### Methods

#### Thermogravimetry Analysis (TGA)

Thermogravimetric (TG) analysis was carried out using a thermogravimetric analyser (Perkin Elmer Pyris 1). The analyser detects the mass loss with a resolution of 0.1 mg as a function of temperature. The samples (3 to 6 mg) were evenly and loosely distributed on the open sample pan. This small amount was taken in order to ensure the uniformity of temperature of the sample with a good reproducibility. Temperature change was controlled from room temperature (25 °C) to 700 °C at six different heating rates of 5, 10, 15, 20, 30, and 40 °C/min in a high purity nitrogen atmosphere (>99.5% nitrogen) at a flow rate of 20 mL/min. Heating rates of 5 to 40 °C were chosen, as higher heating rates are likely to produce too low activation energy due to heat transfer problem (Wielage *et al.* 1999). The sample mass, particle size, and gas flow rate were fixed depending on the experiences and previous publications (Martin *et al.* 2010; Sathasivam

and Haris 2012) for reproducing the results. Before starting each run, nitrogen was used to purge the furnace for 30 min to establish an inert environment in order to prevent any unwanted oxidative decomposition. Different heating rates were used to calculate the activation energy; however, only the 10 °C/min heating rate was considered for decomposition analysis to yield the maximum temperature decomposition peak as reported by many authors (Elkhaoulani *et al.* 2013; Elega *et al.* 2013). TG curves were carefully smoothed at a smoothing region width of 0.2 °C by using a least squares smoothing method, and analyzed by using Pyris 1 software from the TG analyzer. Activation energy was calculated by using MS Excel software according to iso-conversional model-free methods. There were two repetitions for each experiment to verify the reproducibility of obtained mass loss curves. Two sample runs were done under the same experimental conditions for each kind of fibre at each selected heating rate. The weight loss curves were recorded and considered acceptable if they overlapped from two separate tests; otherwise they continued until it overlapped.

## RESULTS AND DISCUSSION

### Decomposition Process of Biomass Fibres

Figures 1 and 2 show the TGA and DTG curves, respectively, of various plant fibres starting at room temperature (25 °C) to 700 °C in a nitrogen environment at the 10 °C/min heating rate. The thermal decomposition of plant fibres consisted of two decomposition steps, except for BPS where there were three steps of degradation. Brigida *et al.* (2010) also reported the same decomposition steps when they used green coconut fibre and banana pseudo-stem, respectively. The first stage of decomposition was the evaporation of moisture where the temperature ranged from 30 °C to 85 °C. As the fibre was heated, the weight of the material decreased via a release of the bound water and volatile extractives. This phenomenon is common for plant fibres and makes the fibre more flexible and easy to collapse, as well as improving the heat transfer rate (Ndazi *et al.* 2006). However, the structurally bound water molecules are resistant to complete water removal during drying due to the hydrophilic nature of plant fibres. The mass loss varied within the range 5 to 10% for all the fibres. White *et al.* (2011) found similar mass loss during evaporation of moisture when they studied different agricultural plant fibres. The greatest mass loss (around 10%) was observed for SCB fibres at this stage.

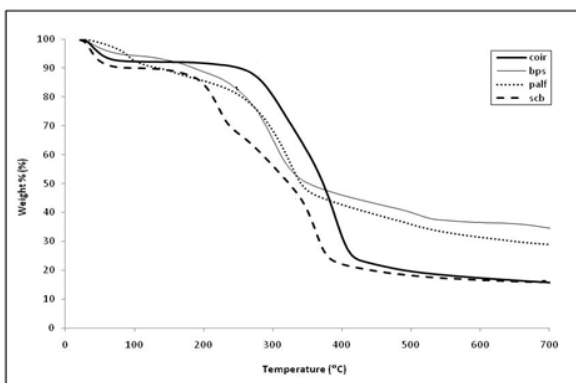


**Fig. 1.** Thermogravimetric analysis (TG) curves for COIR, BPS, PALF, and SCB fibers

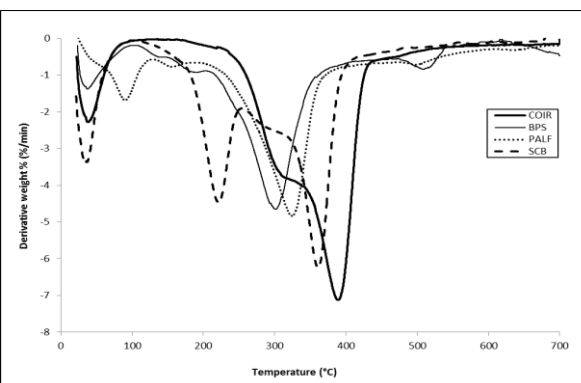


**Fig. 2.** Derivative thermogravimetric (DTG) curves for COIR, BPS, PALF, and SCB fibers

The second phase consisted of hemicellulose decomposition. Hemicelluloses started to decompose at temperatures as low as 145 °C for PALF fibre; however, COIR fibres decomposed at the highest temperature, 301 °C. SCB fibres had the highest mass loss (around 29%) compared to other fibres. This might be because of the higher cellulose content of SCB fibres (Cheng *et al.* 2008) compared to the other fibres. The presence of acetyl groups in hemicelluloses may be responsible for its lower thermal stability, such that the hemicelluloses degrade more quickly compared to other chemical components, *i.e.* the lignin and cellulose present in the fibres. As the temperature increases, chemical changes take place in components of the hemicelluloses due to the cellular breakdown. The result of this study is consistent with other previous studies (Wielage *et al.* 1999; Kim and Eom 2001; Yang *et al.* 2007), and it has been reported that hemicelluloses would decompose within a temperature range between 180 and 350 °C. Compared to hemicelluloses, cellulose is more thermally stable because of its crystalline nature in which it is bonded together by hydrogen bonds to form microfibrils. The samples showed major mass loss (30 to 50%) at  $\geq 300$  °C due to the decomposition of cellulose and lignin. According to Ishak *et al.* (2012), this stage corresponds to the degradation of crystalline cellulose, as the small portion of amorphous cellulose generally degraded in the earlier stage. The DTG graph showed that crystalline cellulose was degraded between the temperatures of 290 and 368 °C. Similar results were also reported by Manfredi *et al.* (2006) and Kim and Eom (2001), where the critical temperature for decomposition of crystalline cellulose was found to be 320 °C.

Lignin was the most difficult component to decompose compared to other components, where the decomposition occurred slowly under the whole temperature range up to 700 °C. According to Yang *et al.* (2007), although the decomposition of lignin could start as early as 160 °C, it decomposed slowly and extended its temperature as high as 900 °C. The DTG curves of COIR, PALF, and SCB fibres reached the equilibrium state where the decomposition occurred slowly under the whole temperature range and therefore, was unidentifiable as individual peaks. However, BPS fibres showed a different trend where there was a significant lignin decomposition peak that reached its maximum decomposition at 502 °C. According to Paiva and Frollini (2006), this was the result of breaking the protolignin bonds that are present in the fibres. This confirmed that the decomposition of lignin occurred in a wider temperature range than that of hemicelluloses and cellulose. These decomposition results were in agreement with other types of natural plant fibres, as reported by Ouajai and Shanks (2005). Lignin is composed of polysaccharides and heavily cross-linked molecules, making it difficult to decompose during thermal degradation. Comparison on onset degradation of all the fibres indicated that PALF and BPS fibres started to degrade at lower temperatures compared to COIR and SCB, which indicated the lesser thermal stability of PALF and BPS. According to Summerscales *et al.* (2010), degradation at lower than 200 °C would limit the choice of that fibre as a reinforcement polymer in composites. John and Thomas (2008) mentioned that the thermal degradation temperature of reinforcement polymer should be higher than 250 °C.

Table 2 shows the thermal degradation data of all four fibre types, where  $T_0$  is the onset temperature at which degradation starts, and  $T_1$ ,  $T_2$ , and  $T_3$  are decomposition temperatures that appear as shoulders in the TGA and as peaks in the DTG graph.

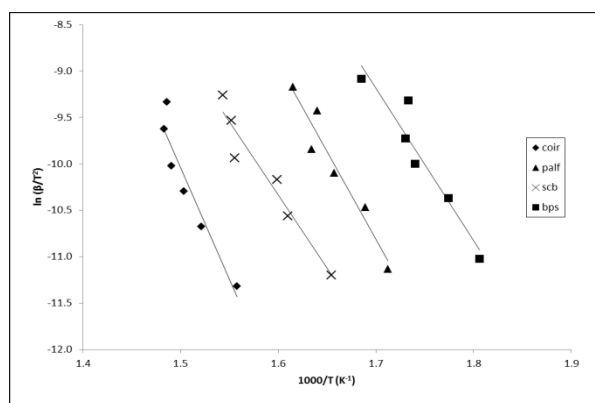
**Table 2.** Thermal Degradation Data and Residual Weight of Plant Fibres at 10 °C/min in Nitrogen Atmosphere

Fibre	$T_0$ (°C)	$T_1$ (°C)	$T_2$ (°C)	$T_3$ (°C)	Residue at 700°C (%)
COIR	228.6	305.9	384.1	-	15.9
BPS	144.2	177.8	296.2	500.9	34.4
PALF	128.7	147.7	319.8	-	28.9
SCB	167.0	216.9	357.1	-	16.1

After 700 °C, only ash and char were left, and the remaining mass was 16% for COIR and SCB whilst 34% and 29% for BPS and PALF, respectively. The differences in the amount of char between the fibres can be attributed to the various chemical compositions in the fibres. It was reported by Reed and Williams (2004) that a high lignin content of natural fibres produced higher levels of char during pyrolysis. The lignin content of COIR was significantly higher compared to other fibres, but in contrast, the char content was the highest in BPS (Khalil *et al.* 2007). This higher value of char in BPS fibres may be due to the combination of higher lignin and hemicelluloses content in BPS fibres.

### Activation Energy

Different heating rates (5, 10, 15, 20, 30, and 40 °C) were considered in kinetic studies to avoid the compensation effects for estimating the kinetic constants as were reported by Ouajai and Shanks (2005). Kinetic analysis was done according to three methods (Kissinger, FWO, and Friedman) for only the major degradation process ranging from 250 to 400 °C. Curves derived from 5 to 40 °C/min heating rates were used in the analysis. Figure 3 show the plots for the Kissinger method and Table 3 presents the activation energy ( $E_a$ ) values for COIR, BPS, PALF, and SCB, respectively. COIR showed the highest activation energy (200 kJ/mol) among the studied fibres, followed by PALF, BPS, and SCB.

**Fig. 3.** Linear plots of  $\ln(\beta/T^2)$  versus  $1000/T$  for various fibers in Kissinger methods**Table 3.** Apparent Activation Energy of Selected Fibres Calculated by Kissinger Method

Fibre	$E_a$ (kJ/mol)	$R^2$
COIR	200.47	0.9088
BPS	136.68	0.9105
PALF	157.09	0.9309
SCB	132.57	0.9359

The conversion values ranged between 20 and 80 wt%, and these values were used for calculating the activation energy of the plant fibres by the F-W-O method. In this method, a series of TG measurements were done at six different heating rates ( $\beta$ ) to each fixed degree of conversion ( $\alpha$ ) and correspondent temperature ( $T$ ).

The standard deviation values were calculated and results are given in Table 4. The  $E_a$  values were calculated from the slope of the plot of  $\log \beta$  vs.  $1000/T$  (Fig. 4). All the slopes corresponded to  $E/R$  for each conversion ( $\alpha = 0.2$  to  $0.8$ ). Figure 4 shows that the fitted lines for all fibres are almost parallel to each other, which implies the possibility of a single reaction mechanism. However, the line was not parallel for BPS ( $\alpha=0.8$ ) (Fig. 4b).

According to Yao *et al.* (2008), the reaction mechanism was changed during higher conversion by the complex reactions in the decomposition process of the main fibre constituents. The activation energy calculated by F-W-O method for COIR, BPS, PALF, and SCB are given in Table 4.

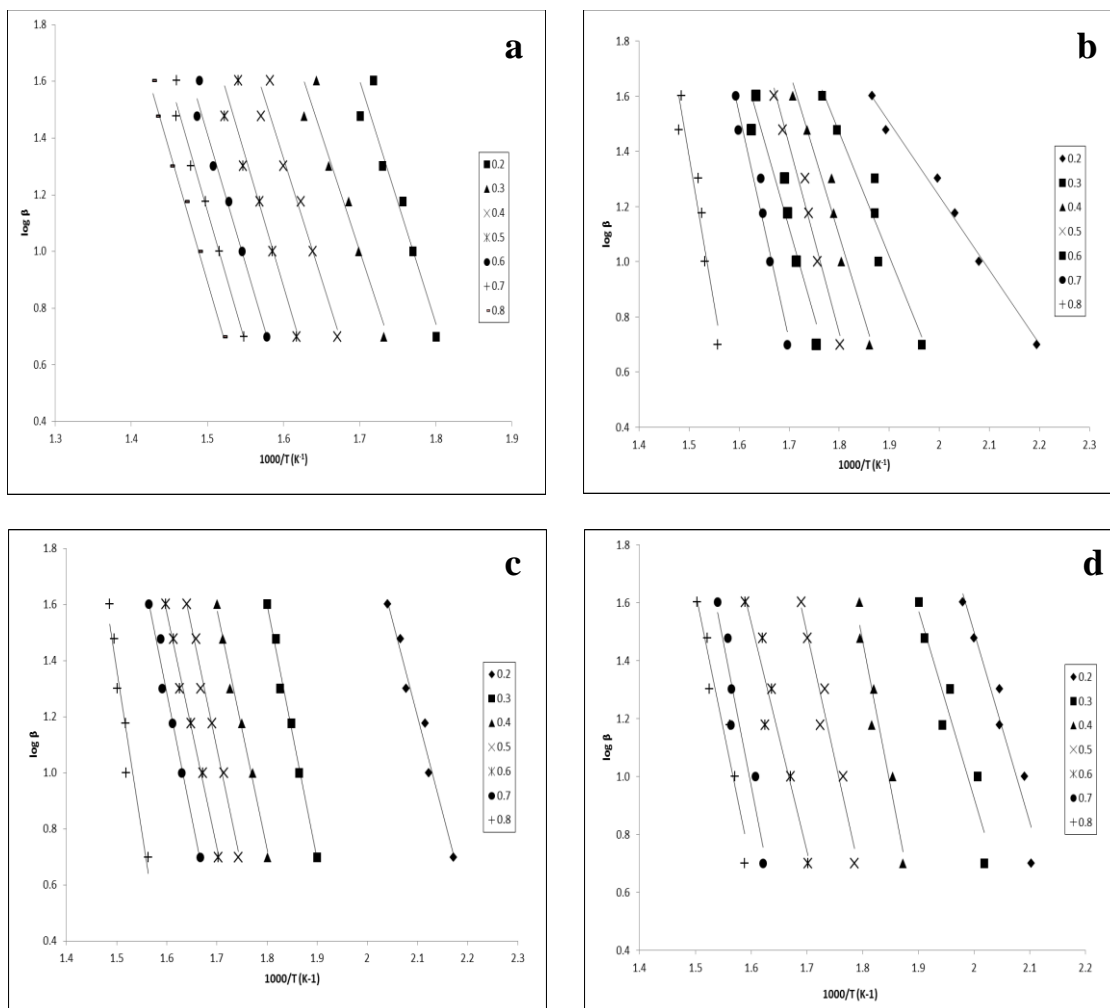


**Fig. 4.** Linear plots of  $\log \beta$  versus  $1000/T$  for various fibers in Flynn-Wall-Ozawa (F-W-O) methods at varying conversions: a) COIR b) BPS c) PALF and d) SCB

**Table 4.** Activation Energies of Plant Fibres Obtained by FWO and Friedman Method

Biomass	F-W-O Method		Friedman Method	
	$E_a$ (kJ/mol)	$R^2$	$E_a$ (kJ/mol)	$R^2$
COIR	104.15 (9.03)	0.9486 (0.0330)	100.04 (8.82)	0.9603 (0.0320)
BPS	75.93 (34.80)	0.9490 (0.9267)	80.79 (37.39)	0.9563 (0.0223)
PALF	94.98 (23.51)	0.9725 (0.0255)	96.28 (20.83)	0.9757 (0.0236)
SCB	89.48 (22.80)	0.9262 (0.0148)	92.87 (27.92)	0.9502 (0.0237)

\* Value in parentheses refers to standard deviation

The highest activation energy was found for COIR (104.2 kJ/mol) followed by PALF, SCB, and BPS. A similar trend of activation energy for different fibres was also found from the Kissinger method. Activation energies for COIR, BPS, PALF, and SCB were also calculated according to the Friedman method (Fig. 5) over a range of conversion ( $\alpha=0.2$  to 0.8), and the calculated results are summarised in Table 4.

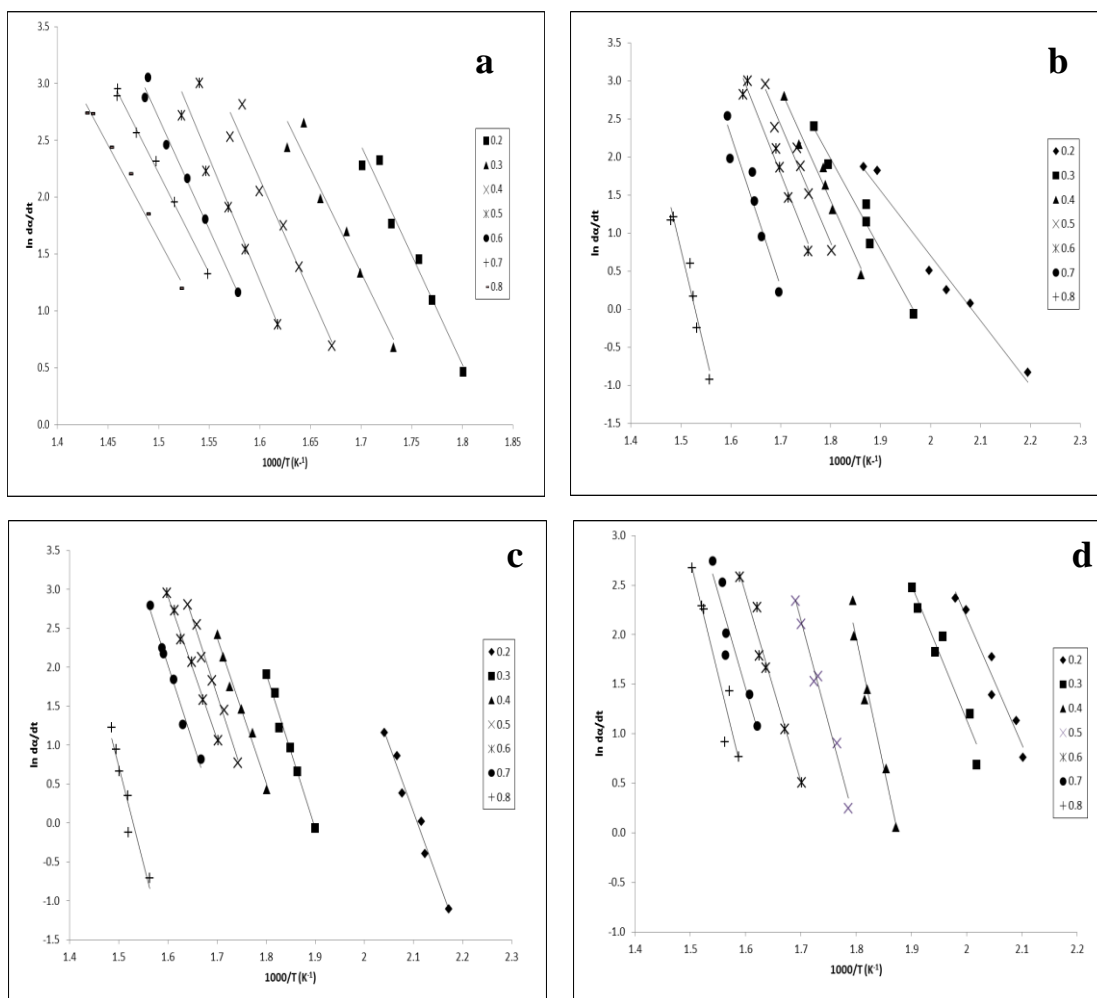


**Fig. 5.** Linear plots of  $\ln(da/dt)$  versus  $1000/T$  for various fibers in Friedman methods: a) COIR b) BPS c) PALF and d) SCB

From Fig. 5 it is clear that the fitted lines at different conversions for COIR, BPS, and PALF are almost parallel with each other, implying the possibility of a single reaction mechanism. However, the lines are not parallel for SCB (Fig. 5b), thereby indicating the complexity of the decomposition mechanism. The mean activation energy calculated by using Friedman method for COIR, BPS, PALF, and SCB were 100.04, 80.79, 96.28, and 92.87 kJ/mol, respectively. The activation energy followed the order COIR>PALF> SCB>BPS, as in the case of the F-W-O method, though there was a discrepancy in activation energy values. However, the mean activation energy was slightly higher in the Kissinger method compared to the other two methods. Brown *et al.* (2000) suggested that these different methods for kinetic analysis are complementary rather than competitive. Fibre is an anisotropic material, and the amount of its principal component, as well as inorganic components varies with geographical location, types of species, and complexity of growth; these variables directly affect the degradation process as well as the activation energy. However, despite these factors, the four types of fibres showed very similar thermal behaviours.

The range of activation energies calculated by all three methods for the four different types of fibres was 75.93 to 200.47 kJ/mol. Values with a similar range were also reported by other researchers for sugarcane bagasse (Aboyade *et al.* 2011), banana fibres (Sathasivam and Haris 2012), caroa, curaua, piassava, and sponge (d'Almeida *et al.* 2008), bamboo, cotton, hemp, jute, kenaf, and rice husk (Yao *et al.* 2008). The variability of the kinetic parameters depends on the nature of plant fibres and the different kinetic methods used. Although the values are in a large range, all three model-free methods indicated that COIR has the highest activation energy compared to other studied fibres. High values of activation energy indicated that COIR is more thermally stable because more energy is needed for the reaction (degradation) process of this fibre compared to others (Van De Velde and Kiekens 2002).

## CONCLUSIONS

1. This study showed that thermal decomposition of the SCB, COIR, PALF, and BPS fibres proceeded in either two or three steps due to hemicelluloses, cellulose, and lignin decomposition. It was observed that the studied fibres showed thermal stability up to 200 °C as the mass loss of all samples was small within the low temperature range.
2. The activation energies of COIR, BPS, PALF, and SCB were 200, 137, 157, and 133 kJ/mol, respectively, when calculated by the Kissinger method. This variation was attributable to the differences in chemical composition of fibres. For the other two methods, the activation energy was lower than these values.
3. The results concluded that COIR was the most thermally stable fibre, followed by PALF, BPS, and SCB, which might be related to the higher lignin content of COIR.

## ACKNOWLEDGMENTS

The authors would like to thank Universiti Sains Malaysia (USM), Penang, Malaysia, for providing Research Grant no. FRGS-203/PTEKIND/6711325 for this study.

## REFERENCES CITED

- Aboyade, A. O., Hugo, T. J., Carrier, M., Meyer, E. L., Stahl, R., Knoetze, J. H., and Görgens, J. F. (2011). "Non-isothermal kinetic analysis of the devolatilization of corn cobs and sugar cane bagasse in an inert atmosphere," *Thermochim. Acta* 517(1), 81-89.
- Brígida, A., Calado, V., Gonçalves, L., and Coelho, M. (2010). "Effect of chemical treatments on properties of green coconut fiber," *Carbohyd. Polym.* 79(4), 832-838.
- Brown, M., Maciejewski, M., Vyazovkin, S., Nomen, R., Sempere, J., Burnham, A., Opfermann, J., Strey, R., Anderson, H. L., Kemmler, A., Keullers, R., Janssens, J., Desseyn, H. O., Li, C., -R., Tang, T. B., Roduit, B., Malek, J., and Mitsuhashi, T. (2000). "Computational aspects of kinetic analysis: Part A: The ICTAC kinetics project-data, methods and results," *Thermochim. Acta* 355(1), 125-143.
- Cabrales, L., and Abidi, N. (2010). "On the thermal degradation of cellulose in cotton fibers," *J. Therm. Anal. Calorim.* 102(2), 485-491.
- Corradini, E., Teixeira, E., Paladin, P., Agnelli, J., Silva, O. R., and Mattoso, L. H. (2009). "Thermal stability and degradation kinetic study of white and colored cotton fibers by thermogravimetric analysis," *J. Therm. Anal. Calorim.* 97(2), 415-419.
- Cheng, K. K., Cai, B.Y., Zhang, J. A., Ling, H. Z., Zhou, Y. J., Ge, J.P., and Xu, J. M. (2008). "Sugarcane bagasse hemicellulose hydrolysate for ethanol production by acid recovery process," *Biochem. Eng. J.* 38(1), 105-109.
- d'Almeida, A., Barreto, D., Calado, V., and d'Almeida, J. (2008). "Thermal analysis of less common lignocellulose fibers," *J. Therm. Anal. Calorim.* 91(2), 405-408.
- Elega, R. G., Djemia, P., Tingaud, D., Chauveau, T., Maniongui, J. G., and Dirras, G. F. (2013). "Effects of alkali treatment on the microstructure, composition, and properties of the *Raffia textilis* fiber," *BioResources* 8(2), 2934-2949.
- Elkhaoulani, A., Arrakhiz, F., Benmoussa, K., Bouhfid, R., and Qaiss, A. (2013). "Mechanical and thermal properties of polymer composite based on natural fibers: Moroccan hemp fibers/polypropylene," *Mater. Design* 49, 203-208.
- Fantozzi, F., Laranci, P., Bianchi, M., De Pascale, A., Pinelli, M., and Cadorin, M. (2009). "CFD simulation of a microturbine annular combustion chamber fuelled with methane and biomass pyrolysis syngas: Preliminary results," *Proceedings of the ASME Turbo Expo 2*, pp. 811-822.
- Flynn, J. H., and Wall, L. A. (1966). "A quick, direct method for the determination of activation energy from thermogravimetric data," *J. Polym. Sci. Pol. Lett.* 4(5), 323-328.
- Friedman, H. L. (1964). "Kinetics of thermal degradation of char forming plastics from thermogravimetry. Application to a phenolic plastic," *J. Polym. Sci. Pol. Sym.* 6(1), 183-195.

- Goh, C. S., Tan, K. T., Lee, K. T., and Bhatia, S. (2010). "Bio-ethanol from lignocellulose: status, perspectives and challenges in Malaysia," *Bioresource Technol.* 101(13), 4834-4841.
- Guillain, M., Fairouz, K., Mar, S. R., Monique, F., and Jacques, L. (2009). "Attrition-free pyrolysis to produce bio-oil and char," *Bioresource Technol.* 100(23), 6069-6075.
- Ishak, M., Sapuan, S., Leman, Z., Rahman, M., and Anwar, U. (2012). "Characterization of sugar palm (*Arenga pinnata*) fibres," *J. Therm. Anal. Calorim.* 109(2), 981-989.
- John, M. J., and Thomas, S. (2008). "Biofibres and biocomposites," *Carbohydr. Polym.* 71(3), 343-364.
- Khalil, H. P. S. A., Alwani, M. S., and Omar, A. K. M. (2007). "Chemical composition, anatomy, lignin distribution, and cell wall structure of Malaysian plant waste fibers," *BioResources* 1(2), 220-232.
- Kim, H. J., and Eom, Y. G. (2001). "Thermogravimetric analysis of rice husk flour for a new raw material of lignocellulosic fiber-thermoplastic polymer composites," *Mokchae Konghak* 29(3), 59-67.
- Kissinger, H. E. (1957). "Reaction kinetics in differential thermal analysis," *Anal. Chem.* 29(11), 1702-1706.
- Lu, C., Song, W., and Lin, W. (2009). "Kinetics of biomass catalytic pyrolysis," *Biotechnol. Advan.* 27(5), 583-587.
- Manfredi, L. B., Rodríguez, E. S., Wladyka-Przybylak, M., and Vázquez, A. (2006). "Thermal degradation and fire resistance of unsaturated polyester, modified acrylic resins and their composites with natural fibres," *Polym. Degrad. Stabil.* 91(2), 255-261.
- Martin, A. R., Martins, M. A., da Silva, O. R. R. F., and Mattoso, L. H. C. (2010). "Studies on the thermal properties of sisal fiber and its constituents," *Thermochimica Acta* 506, 14-19.
- Mothé, C. G., and de Miranda, I. C. (2009). "Characterization of sugarcane and coconut fibers by thermal analysis and FTIR," *J. Therm. Anal. Calorim.* 97(2), 661-665.
- Munir, S., Daood, S. S., Nimmo, W., Cunliffe, A. M., and Gibbs, B. M. (2009). "Thermal analysis and devolatilization kinetics of cotton stalk, sugar cane bagasse and shea mea under nitrogen and air atmospheres," *Bioresource Technol.* 100, 1413-1418.
- Ndazi, B., Tesha, J., and Bisanda, E. (2006). "Some opportunities and challenges of producing bio-composites from non-wood residues," *J. Mater. Sci.* 41(21), 6984-6990.
- Opfermann, J., Kaisersberger, E., and Flammersheim, H. (2002). "Model-free analysis of thermoanalytical data-advantages and limitations," *Thermochim. Acta* 391(1), 119-127.
- Ouajai, S., and Shanks, R. (2005). "Composition, structure and thermal degradation of hemp cellulose after chemical treatments," *Polym. Degrad. Stabil.* 89(2), 327-335.
- Paiva, J. M., and Frollini, E. (2006). "Unmodified and modified surface sisal fibers as reinforcement of phenolic and lignophenolic matrices composites: Thermal analyses of fibers and composites," *Macromol. Mater. Eng.* 291(4), 405-417.
- Reed, A. R., and Williams, P. T. (2004). "Thermal processing of biomass natural fibre wastes by pyrolysis," *Int. J. Energ. Res.* 28(2), 131-145.
- Sathasivam, K., and Haris, M. R. H. M. (2012). "Thermal properties of modified banana trunk fibers," *J. Therm. Anal. Calorim.* 108(1), 9-17.

- Sbirrazzuoli, N., Vincent, L., Mija, A., and Guigo, N. (2009). "Integral, differential and advanced isoconversional methods: Complex mechanisms and isothermal predicted conversion–time curves," *Chemometr. Intell. Lab.* 96(2), 219-226.
- Slopiecka, K., Bartocci, P., and Fantozzi, F. (2012). "Thermogravimetric analysis and kinetic study of poplar wood pyrolysis," *Appl. Energ.* 97, 491-497.
- Sumathi, S., Chai, S., and Mohamed, A. (2008). "Utilization of oil palm as a source of renewable energy in Malaysia," *Renew. Sus. Energ. Rev.* 12(9), 2404-2421.
- Summerscales, J., Dissanayake, N. P., Virk, A.S., and Hall, W. (2010). "A review of bast fibres and their composites. Part 1–Fibres as reinforcements," *Compos. Part A-Appl. S.* 41(10), 1329-1335.
- Van De Velde, K., and Kiekens, P. (2002). "Thermal degradation of flax: The determination of kinetic parameters with thermogravimetric analysis," *J. Appl. Polym. Sci.* 83(12), 2634-2643.
- White, J. E., Catallo, W. J., and Legendre, B. L. (2011). "Biomass pyrolysis kinetics: A comparative critical review with relevant agricultural residue case studies," *J. Anal. Appl. Pyrol.* 91(1), 1-33.
- Wielage, B., Lampke, T., Marx, G., Nestler, K., and Starke, D. (1999). "Thermogravimetric and differential scanning calorimetric analysis of natural fibres and polypropylene," *Thermochim. Acta* 337(1), 169-77.
- Yang, H., Yan, R., Chen, H., Lee, D. H., and Zheng, C. (2007). "Characteristics of hemicellulose, cellulose and lignin pyrolysis," *Fuel* 86(12), 1781-1788.
- Yao, F., Wu, Q., Lei, Y., Guo, W., and Xu, Y. (2008). "Thermal decomposition kinetics of natural fibers: Activation energy with dynamic thermogravimetric analysis," *Polym. Degrad. Stabil.* 93(1), 90-98.

Article submitted: September 25, 2013; Peer review completed: November 2, 2013;  
Revised version received: November 6, 2013; Accepted: November 7, 2013; Published:  
November 13, 2013.